

EFFECT OF LIGHT INDUCED DEGRADATION ON PASSIVATING PROPERTIES OF A-SI:H LAYERS DEPOSITED ON CRYSTALLINE SI

S. Olibet, E. Vallat-Sauvain, C. Ballif

Institute of Microtechnology (IMT), University of Neuchâtel

Breguet 2, 2000 Neuchâtel Switzerland, phone: +41 32 718 33 18, fax: +41 32 718 32 01, email: sara.olibet@unine.ch

ABSTRACT: Passivation properties of intrinsic hydrogenated amorphous silicon (i a-Si:H) layers on n- and p-type doped monocrystalline silicon (c-Si) are studied in two thickness series. The effect of light soaking on the passivation performance of a-Si:H i-layers of varying thicknesses are evaluated. Within the thickness series, optimized i a-Si:H layers show very good passivation properties (S_{eff} as low as 18 cm/s at an injection level of 10^{15}cm^{-3} is achieved) for n- as well as for p-type c-Si. Surprisingly these properties are not affected as expected by light soaking. The measured injection level dependence of the effective surface recombination velocity is modeled by considering recombination through amphoteric defects, characteristic of a-Si:H. Finally, heterojunction devices incorporating the thinnest passivation layer show maximum open circuit voltage (V_{OC}) as high as 713mV. A best solar cell conversion efficiency of 17.6% with a V_{OC} of 705mV is achieved on small area cell on flat n-type wafer. On p-type wafer, a V_{OC} of 690mV and efficiency of 16.3% is achieved.

Keywords: Passivation, Stability, Heterojunction

1 INTRODUCTION

Surface passivation of crystalline silicon (c-Si) leads to a minimal value of the recombination rate of photogenerated carriers at the c-Si surface. This is commonly achieved by a) minimizing surface recombination center density and/or b) minimizing photogenerated carrier recombination probability by field effect. Among various passivation layers, a-Si:H has proven to be a very efficient material. The aim of this work is to study the effect of light soaking on the passivation quality of such a-Si:H layers.

The effect of light soaking on a-Si:H is well known: it leads to an increased recombination center density (dangling bonds) and consequently to a degradation of the material's electronic quality. The resulting degradation of performance of amorphous silicon solar cells depends on the thickness of the intrinsic a-Si:H layer, that is, on the total free carrier recombination rate that increases with i-layer thickness. P-i-n devices with thin i-layers are therefore more stable because of their more efficient carrier extraction.

In order to quantify the effect of light soaking on passivation properties, thickness series of a-Si:H i-layers ranging from 5 to 500nm are deposited by VHF-PECVD (very-high frequency plasma enhanced chemical vapor deposition) on both surfaces of lightly doped n- and p-type FZ c-Si substrates.

In this work, we show that, for n- as well as for p-type substrates, the effective surface recombination velocity (S_{eff}) is i-layer thickness dependent. The best (minimal) value of $S_{\text{eff}}=18\text{cm/s}$ is measured for i-layers with thicknesses around 40nm. Surprisingly S_{eff} does not degrade as expected under standard light soaking (AM1.5, 50°C) conditions. The observed variations are thickness-dependent: the thinnest layer is the less stable one, but we find that degradation in dark conditions shows comparable tendencies.

These results will be discussed by taking into account recombination through amphoteric defects characteristic for a-Si:H. In this model, the density of recombination centers is thickness dependent, and their average state of charge is considered to be induced by the free a-Si:H surface potential.

Finally heterojunction devices incorporating optimized a-Si:H i-layers are fabricated. Non-contacted heterojunction structures consisting of wafers passivated on both sides with i a-Si:H and a-Si:H doped layer (p-a-Si:H/i-a-Si:H/n-c-Si/i-a-Si:H/p-a-Si:H) show S_{eff} value as low as 7cm/s, with a predicted maximal V_{OC} of 718mV on n-type c-Si. After contacting both sides for current extraction, the resulting solar cell shows effectively V_{OC} value as high as 713mV close to the record value of 730mV reported by [1].

2 EXPERIMENTAL

2.1 Passivation layers

In this work double side polished 60Ωcm n-type and 130Ωcm p-type FZ silicon wafers of 300 resp. 525μm thickness are used as substrates. Prior to a-Si:H deposition the wafers are just taken out of box and immersed in diluted HF to remove the native oxide on top of them.

Intrinsic a-Si:H passivation layers are deposited by VHF-PECVD on both surfaces. The layers have thicknesses in the range from 5 to 500nm, measured with a profilometer and a spectroscopic ellipsometer. Their fully amorphous nature is verified by transmission electron microscopy (TEM).

The deposition conditions are a plasma excitation frequency of 70MHz, a substrate temperature of 180°C, a chamber pressure of 0.4mbar and silane concentration ($SC=[\text{SiH}_4]/[\text{SiH}_4+\text{H}_2]$) of 28%, yielding device-quality i a-Si:H material. Then samples are annealed for 1h30min at a temperature of 180°C under nitrogen flow.

Light soaking is performed under AM1.5 spectra at a temperature of 50°C in ambient atmosphere (typical a-Si:H light soaking conditions). Dark degradation is carried out in ambient atmosphere in a drawer at about 22°C.

2.2 Lifetime measurements

To determine the quality of c-Si surface passivation, the effective carrier lifetime (τ_{eff}) is measured by the quasi-steady-state photoconductance (QSSPC) method,

using a commercial WCT-100 photoconductance set-up from Sinton Consulting [2]. This contactless measurement technique permits to measure τ_{eff} over a wide range of c-Si bulk injection level ($\Delta n = \Delta p$). In this study, infinite bulk lifetime is assumed. Thus, as both surface of the c-Si substrates are passivated by using the same i-layers, the expression for the upper bound for the real value of S_{eff} becomes $S_{\text{eff}} = W/2 \cdot 1/\tau_{\text{eff}}$, where W is the c-Si wafer thickness [3].

2.3 Modeling

The effective surface recombination velocity S_{eff} is defined as $S_{\text{eff}} = U_s/\Delta n$ where $\Delta n (= \Delta p)$ is the excess photogenerated minority carrier density in the bulk of the c-Si wafer and U_s the surface recombination rate. According to [3], starting from the charge neutrality condition fulfillment in the complete system, a model for surface recombination under band bending conditions at the c-Si surface is developed. We use the same approach for modeling recombination at the a-Si:H/c-Si interface but replace Shockley-Read-Hall recombination (U_{SRH}) by dangling bond recombination (U_{DB}) typical for a-Si:H. In this situation, sketched in Fig. 1, the dangling bonds, with their amphoteric character (i.e. three possible charge states denoted D^0 for neutral, D^+ for positively and D^- for negatively charged) act as recombination centers. Depending on the charge induced potential at the free surface of the a-Si:H layer, the amphoteric recombination centers at the interface possess a total positive or negative charge density. Therefore the charge neutrality condition can be written as $Q_{\text{Si}} + Q_{\text{DB}} + Q_i = 0$.

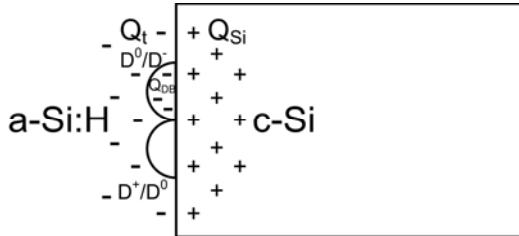


Figure 1: Sketch of the a-Si:H recombination model used for the modeling of a-Si:H/c-Si interface recombination. The dangling bonds act as three-valued recombination centers: positively ionized D^+ , negatively ionized D^- and neutral D^0 dangling bonds. In the present sketch, a negative charge Q_i in a-Si:H induces negatively charged dangling bonds at the a-Si:H/c-Si interface.

According to [4], the expression for the recombination rate becomes

$$U_{\text{DB}} = \frac{1}{\tau_p^0} \cdot \left(\frac{\sigma_n^0}{\sigma_p^0} \cdot n_s + p_s \right) \left(\frac{p_s \cdot \sigma_p^0}{n_s \cdot \sigma_n^+} + 1 + \frac{n_s \cdot \sigma_n^0}{p_s \cdot \sigma_p^-} \right)$$

where n_s and p_s are the densities of free photogenerated electrons and holes at the a-Si:H/c-Si interface, and $\tau_i^j = (v_{\text{th}} \sigma_i^j N_{\text{DB}})^{-1}$ are the free carriers ‘‘capture times’’: N_{DB} is the total density of dangling bonds at the interface (in cm^{-2}), σ_i^j is the capture cross section for the capture of the carrier i (n_s or p_s) on a dangling bond in the state of charge j (+, -, or 0) and v_{th} is the thermal velocity. Beck [5] found a electron/hole capture cross section ratio of $\sigma_n^0/\sigma_p^0 \approx \mu_n^0/\mu_p^0$ where μ is the band mobility. σ_n^0/σ_p^0 is therefore supposed to be about 10 [6]. According to

Hubin [6], the ratio of charged to neutral capture cross sections σ_n^+/σ_n^0 and σ_p^-/σ_p^0 are equal, however with values that range from 1 to 1000 depending on the author.

3 RESULTS

3.1 Thickness series

Fig. 2 shows the thickness dependence of the passivating properties of a-Si:H i-layers deposited on both sides of the n- and p-type c-Si substrates. S_{eff} is measured directly after initial annealing of the samples.

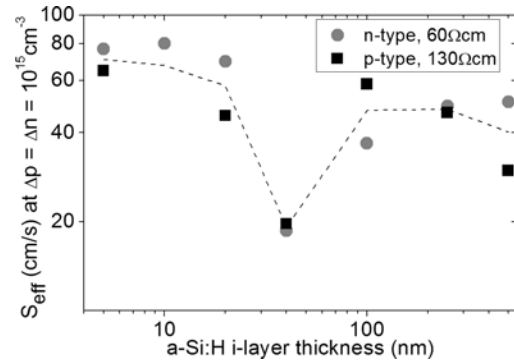


Figure 2: a-Si:H i-layer thickness dependent surface passivation of n- and p-type c-Si substrates. S_{eff} is evaluated directly after initial annealing by the QSSPC technique at $\Delta p = \Delta n = 10^{15} \text{cm}^{-3}$. The dashed line is a guide to the eyes.

3.2 Light soaking studies

The effect of light soaking on the normalized surface recombination velocity $S_{\text{eff}}/S_{\text{effann}}$ for a selection of a-Si:H i-layer thickness of 5nm, 40nm and 500nm on n-type c-Si (60 Ohm cm) is shown in Fig. 3. Same trend is observed for i a-Si:H passivated p-type c-Si (130 Ohm cm) substrates.

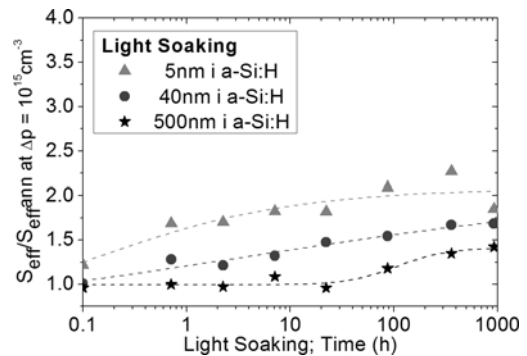


Figure 3: Averaged S_{eff} at $\Delta p = 10^{15} \text{cm}^{-3}$, normalized to its initial value as a function of light soaking time for samples of the thickness series given in Fig. 1 for i a-Si:H passivating layers on n-type c-Si. Dashed lines are a guide to the eye.

3.3 Dark Degradation studies

Fig. 4 shows the evolution of surface passivation properties as a function of time in the dark for the same layers as in Fig. 3. For direct comparison of dark

degradation and light soaking, results shown in Fig. 3 are represented by the empty symbols. Again, the measured evolutions are irrespective of the wafer-type.

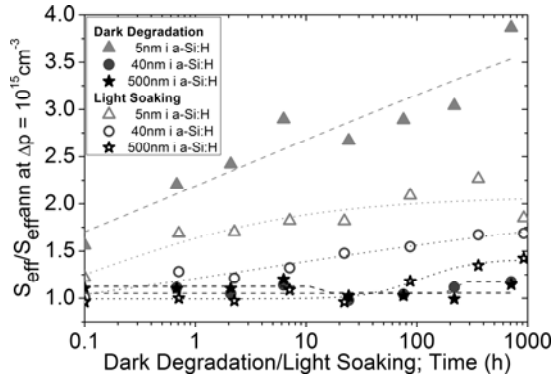


Figure 4: Averaged normalized S_{eff} as a function of dark degradation time (full symbols and dashed lines) for the same i a-Si:H passivation layers of 3 different thickness shown in Fig. 3. For comparison the light soaking behaviour shown in Fig. 3 is indicated by empty symbols and dotted lines.

3.4 Modeling of S_{eff} vs $\Delta n = \Delta p$

Fig. 5 shows the injection level dependence of the surface recombination velocity (i.e. S_{eff} vs $\Delta n = \Delta p$ curves) for n-type as well as p-type c-Si passivated by depositing 5 nm thin a-Si:H i-layers on both surfaces. Best fits to all measured data are obtained for $\sigma_n^0/\sigma_p^0 = 70$ and $\sigma^+/\sigma^0 = 300$. $Q_t + Q_{\text{DB}}$ as well as $\tau_p^0 = (v_{\text{th}}\sigma_p^0 N_{\text{DB}})^{-1}$ are the model variables, whose values, as resulting from the fits, are listed in Table I.

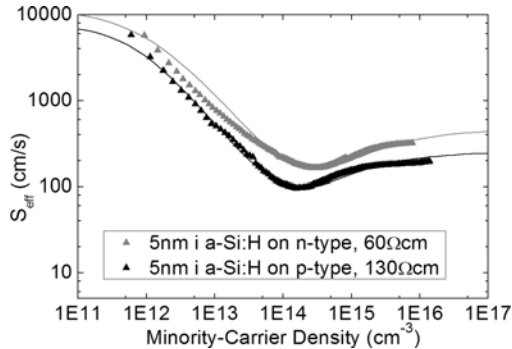


Figure 5: Injection level dependent passivation properties (S_{eff} vs $\Delta p = \Delta n$ curves) of 5 nm thin a-Si:H i-layers on n-type (60 Ωcm) and p-type (130 Ωcm) after 10 h of dark degradation. Measured values are represented by symbols while lines are fit results using parameters from Table I.

Table I: Values of parameters used for the fits in Fig. 5.

sample	τ_p^0 (s)	$Q_t + Q_{\text{DB}}$ (cm^{-2})
n c-Si, 5nm i a-Si:H	0.12	$-2.5 \cdot 10^{10}$
p c-Si, 5nm i a-Si:H	0.22	$-1.7 \cdot 10^{10}$

Fig. 6 shows S_{eff} vs Δp curves as a function of i-layer thickness and as a function of dark degradation time. Both measurements are done on n-type wafers, and the observed trends are identical on p-type wafers.

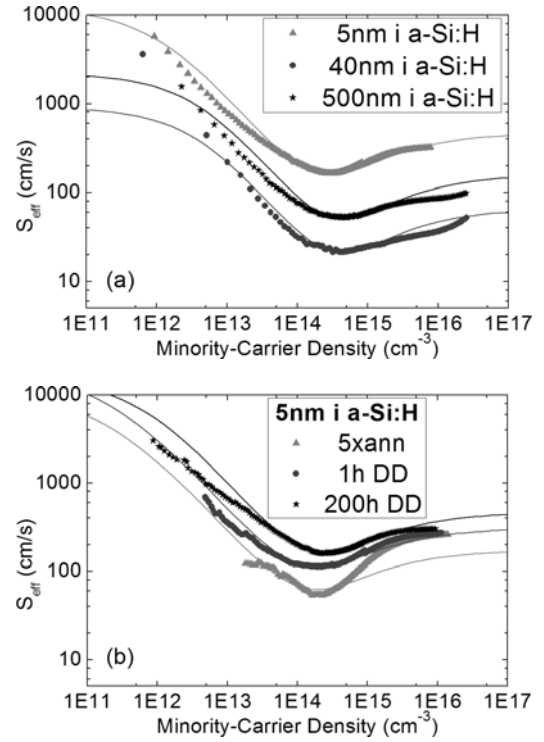


Figure 6: Injection level dependent passivation properties of a-Si:H i-layers on n-type (60 Ωcm) c-Si for (a) a-Si:H i-layer with varying thickness after 10 h of dark degradation and (b) for the thinnest a-Si:H i-layer at different dark degradation times. Symbols show measured values while fits obtained with parameters from Table II are represented by lines.

Table II: Set of parameters used for the fits in Fig. 6.

sample	τ_p^0 (s)	$Q_t + Q_{\text{DB}}$ (cm^{-2})
<i>After 10h dark degradation</i>		
5nm i a-Si:H	0.12	$-2.5 \cdot 10^{10}$
40nm i a-Si:H	0.85	$-3.1 \cdot 10^{10}$
500nm i a-Si:H	0.35	$-3.1 \cdot 10^{10}$
<i>5nm i a-Si:H</i>		
annealed	0.33	$-2.0 \cdot 10^{10}$
1h dark degradation	0.18	$-2.0 \cdot 10^{10}$
200h dark degradation	0.12	$-2.3 \cdot 10^{10}$

3.6 Heterojunction Devices

Finally, in the aim of fabricating amorphous/crystalline silicon heterojunction solar cells, the thinnest of these passivation layers are incorporated between the c-Si and doped a-Si:H layers onto both sides of the wafers resulting thus in $\langle p \rangle$ a-Si:H / $\langle i \rangle$ a-Si:H / $\langle n \rangle$ c-Si / $\langle i \rangle$ a-Si:H / $\langle n \rangle$ a-Si:H heterojunction structures (Note: dopant types inverted for p-type c-Si based heterojunction structures). The wafers used as substrates are double side polished and more doped than the ones used for the passivation series, i.e. 1 Ωcm n-type resp. 0.5 Ωcm p-type FZ.

Non-contacted heterojunction structures are used to study the injection level dependent interface recombination as shown in Fig. 7. Sinton QSSPC measurement of $\tau_{\text{eff}} = 2 \text{ ms}$, yielding a value $S_{\text{eff}} = 7 \text{ cm/s}$ at $\Delta p = 10^{15} \text{ cm}^{-3}$ results in a predicted upper value for the open circuit voltage (V_{oc}) [2] of about 718 mV.

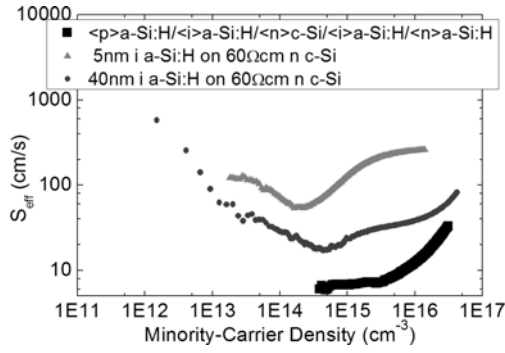


Figure 7: Injection dependent effective surface recombination velocity of non-contacted heterojunction structure based on 1Ωcm n-type, compared to the 60Ωcm n-type sample, with 5 and 40nm thin i-a-Si:H passivation layers exposed to ambient air. The value for S_{eff} of 7cm/s (at $\Delta p=10^{15}\text{cm}^{-3}$) results in a predicted upper value of $V_{\text{OC}}=718\text{mV}$.

The contacted part of the heterojunction device is structured into about 0.2cm^2 area size solar cells with 80nm ITO on front and ITO/Al back reflector. Predicted $V_{\text{OC}}=718\text{mV}$ is almost attained on fully functional devices with 713mV (but efficiency of 16.9%). The corresponding current-voltage (IV) characteristics under AM1.5g spectrum are shown in Fig. 8. The short-circuit current density (J_{SC}), is deduced from the measurement of the external quantum efficiency (EQE), by integrating over the solar spectrum the product of EQE times the flux density of photons for each wavelength. Best conversion efficiency reached now are 17.6% from $\langle p \rangle$ -a-Si:H / $\langle i \rangle$ -a-Si:H / $\langle n \rangle$ -c-Si / $\langle i \rangle$ -a-Si:H / $\langle n \rangle$ -a-Si:H structure and 16.3% from $\langle n \rangle$ -a-Si:H / $\langle i \rangle$ -a-Si:H / $\langle p \rangle$ -c-Si / $\langle i \rangle$ -a-Si:H / $\langle p \rangle$ -a-Si:H structure.

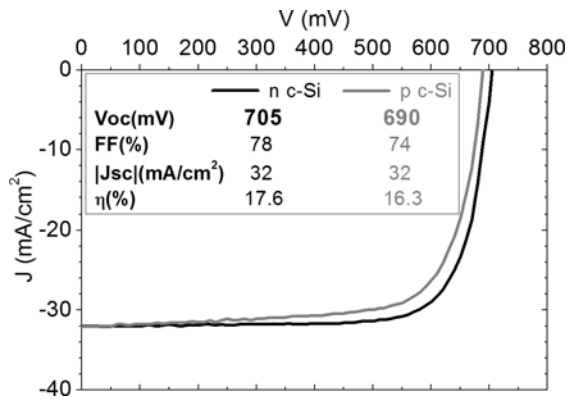


Figure 8: Heterojunction solar cell characteristics based on flat n-type as well as on p-type c-Si.

4 DISCUSSION

Fig. 2 shows that similar passivation performances (i.e. similar S_{eff} values at an injection level of $\Delta n=\Delta p=10^{15}\text{cm}^{-3}$) are achieved on double-sided lightly doped passivated wafers of both n- and p-type. The a-Si:H i-layer thickness has a major effect on the observed S_{eff} value, with a minimal value for i-layer thickness around 40nm. Light soaking of the i-a-Si:H passivated wafers shows small variations of the S_{eff} values (see Fig. 3). The

largest variations are observed for the thinnest passivation layers, whereas it is almost negligible for thick layers. This is in contradiction with the well known Staebler-Wronski effect observed in a-Si:H layers. In a-Si:H, the main metastable defect created by prolonged illumination is the silicon dangling bond, which acts as recombination center. According to [7] the relative increase of N_{DB} exhibits a $t^{1/3}$ dependence on illumination time. Taking for example the 500nm a-Si:H i-layer on p-type c-Si wafer, none of the expected increase of S_{eff} is observed at all as shown in Fig. 9. However, this layer is thick enough to absorb significant light under light soaking conditions and should have suffered an increased “bulk” dangling bond density, which does not affect the value of S_{eff} . As light soaking studies don’t show the expected results, dark degradation is further investigated in order to elucidate the possible cause of the observed variations of S_{eff} in the thinnest passivation layers. After 1000h of light soaking, the initial value of S_{eff} can be recovered by annealing again the samples. From Fig. 4, it can be clearly seen that S_{eff} of the thinnest a-Si:H i-layer degrades even more in the dark than under light soaking conditions. Thus, the light induced creation of metastable defects in the a-Si:H bulk is not the microscopic process governing the observed light and dark degradation kinetics as monitored by the variation of S_{eff} .

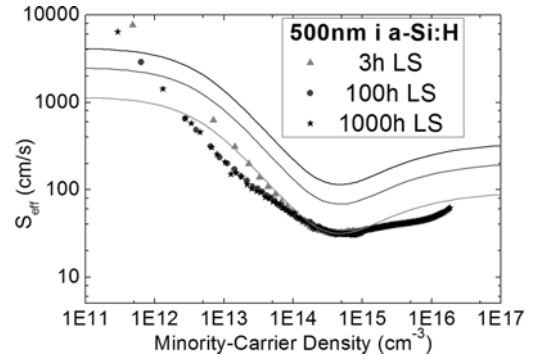


Figure 9: S_{eff} vs Δn curves measured during light soaking of a thick (500 nm) i-a-Si:H passivation layer. The symbols show measured data while lines are calculated S_{eff} vs Δn curves assuming $t^{1/3}$ increasing N_{DB} (“bulk” Staebler-Wronski effect).

In order to gain insight in the mechanism limiting S_{eff} in our structures, the surface recombination model sketched in Fig. 1 is successfully applied to the injection dependence of S_{eff} . In the proposed model, surface recombination occurs via dangling bonds at the a-Si:H/c-Si interface. Good fits are obtained with $\sigma_{\text{n}}^0/\sigma_{\text{p}}^0=70$ and $\sigma^+/\sigma^0=300$ for all cases, and by adjusting the values of τ_{p}^0 (which is inversely proportional to N_{DB}) as well as $Q_{\text{t}}+Q_{\text{DB}}$. All our S_{eff} vs $\Delta n(=\Delta p)$ curves can be fitted with a negative trapped charge within the a-Si:H i-layer (or, equivalently, to a negative free a-Si:H surface potential) and a varying $\tau_{\text{p}}^0=(v_{\text{th}}\sigma_{\text{p}}^0N_{\text{DB}})^{-1}$.

The fits of the S_{eff} vs $\Delta n(=\Delta p)$ curves measured on the two thickness series result in thickness-dependent τ_{p}^0 , while the other fit parameters do not vary significantly. The minimal S_{eff} value observed for a-Si:H i-layer thicknesses around 40nm is related with a minimal N_{DB} value (and maximal τ_{p}^0 as given in Table II). By increasing i-layer thickness from 5 to 40nm, N_{DB} is

reduced by a factor of 20 whereas by further increasing layer thickness (from 40 to 500nm) N_{DB} again increases but this time by a factor of 4. The largest S_{eff} in thin layers can be attributed to the fact that firstly grown a-Si:H layers are more defective than “bulk” a-Si:H layers, whereas the increase of S_{eff} after 40nm could possibly be due to a more defective interface induced by mechanical stress. Indeed, it is observed that 1 μ m thick a-Si:H layers can peel off when deposited on c-Si wafers.

The S_{eff} vs $\Delta n = \Delta p$ curves measured during light soaking are as well fitted with the dangling bond recombination model. The light soaking independent S_{eff} value measured in thick a-Si:H i-layer and increasing S_{eff} values measured in thin layers under illumination as well as in darkness, are attributed in our model to a constant interface dangling bond density. In this interpretation, it would thus seem that even if light soaking creates more dangling bonds in the bulk of the thick a-Si:H i-layers, the interface defect density is not affected by this bulk, post-deposition material degradation. On the other hand, the observed variation of S_{eff} values during dark degradation in thin a-Si:H i-layers can be attributed (from our fits of the corresponding S_{eff} vs $\Delta n = \Delta p$ curves) to an increasing negative charge $Q_t + Q_{DB}$ during exposure to ambient air (under illumination as well as in darkness). This variation is reversible by thermal annealing. Indeed, we observe that the initial value of S_{eff} can also be recovered by dipping the c-Si wafers passivated with a-Si:H i-layers in diluted HF. This confirms that the negative free a-Si:H surface potential (which can be caused by a physisorbed layer forming on top of a-Si:H layers) is responsible for the increasing negative charge of the dangling bonds at the c-Si/a-Si:H interface, and corresponding increasing surface recombination rate.

From our modeling of the S_{eff} vs $\Delta n = \Delta p$ curves measured in the thickness series and during light and dark soaking of our i a-Si:H passivated p- and n-type lightly doped wafers, the emerging picture is that recombination through amphoteric dangling bonds is prevalent in the surface recombination. The co-existence of two recombination paths through dangling bonds, which is strongly affected by the state of charge of the recombination centers may be the decisive effect for minimizing surface recombination of c-Si by i a-Si:H. From this point of view, intrinsic a-Si:H could have some advantages compared to other passivation schemes. For example, it is known that SiN_x yields the best c-Si surface passivation but, when incorporated within a solar cell yields poorer performance due to high Q_t [8]. Furthermore, the fact that SiO_2 layers passivate better n-type than p-type wafers is due to their high ratio of electron to hole capture cross section $\sigma_n/\sigma_p = 100$ [9]. Although the latter can only be observed on highly doped c-Si substrates (i.e. the ones used commonly for the fabrication of heterojunction devices), i a-Si:H passivation is less sensitive to the wafer type (even though its electron/hole capture cross section ratio is almost as high), due to its high charged to neutral capture cross section ratio $\sigma^+/\sigma^0 \gg 1$. Finally, the high, and almost identical, value of V_{OC} achieved in this work on both types of (highly doped) c-Si wafers by depositing the same a-Si:H i-layers bears out our statements.

The impact of the outer i a-Si:H surface potential on the minimization of interface recombination is further evidenced in Fig. 7 where, the lowest S_{eff} value is

obtained for i-layers sandwiched between the c-Si and a p- or n-doped layer.

The functional devices fabricated in this study do not exhibit yet high J_{SC} values (see Fig. 8). This is due to the use of planar wafers, without any light management scheme such as anti reflection layers or surface pyramids. However, we reach V_{OC} and FF values among the best reported for full heterojunction solar cells. The introduction of pyramids is expected to lead to strong current and efficiency increase.

5 CONCLUSIONS

Passivation properties of intrinsic a-Si:H on lightly doped c-Si wafers do not vary significantly under light soaking. The slight observed variations are similar to those observed under dark exposition to ambient conditions. A new physical model taking into account the amphoteric nature of dangling bonds for interface recombination is introduced. It allows calculating the injection dependence of S_{eff} and is able to reproduce observed results on n- and p-type wafers. Furthermore it points out the dependence of the S_{eff} vs $\Delta n (= \Delta p)$ curves on the state of charge of recombination centers. Finally, the incorporation of these optimized a-Si:H layers on flat wafers is used for the fabrication of high- V_{OC} ($V_{OC} = 713$ mV) heterojunction solar cells.

ACKNOWLEDGMENTS

This work is supported by the Swiss National Foundation (FN-200021-107469).

REFERENCES

- [1] E. Maruyama, A. Terakawa, M. Taguchi, Y. Yoshimine, D. Ide, T. Baba, M. Shima, H. Sakata, M. Tanaka, Presented at 4th IEEE World Conference on Photovoltaic Energy Conversion (2006).
- [2] R.A. Sinton, A. Cuevas, Appl. Phys. Lett. 69 (1996) 2510.
- [3] A.G. Aberle, Crystalline Silicon Solar Cells : Advanced Surface Passivation and Analysis, University of New South Wales, Sydney (1999).
- [4] J. Hubin, A.V. Shah, E. Sauvain, Philos. Mag. Lett. 66 (1992) 115.
- [5] N. Beck, N. Wyrsh, Ch. Hof, A. Shah, J. Appl. Phys. 79 (1996) 12.
- [6] J. Hubin, A.V. Shah, E. Sauvain, P. Pipoz, J. Appl. Phys. 78 (1995) 10.
- [7] M. Stutzmann, W.B. Jackson, C.C. Tsai, Phys. Rev. B 32 (1985) 1
- [8] S.W. Glunz et al., Proceedings 20th European Photovoltaic Solar Energy Conference (2005) 572
- [9] A.G. Aberle, S. Glunz, W. Warta, J. Appl. Phys. 71 (1992) 4422-4431